# Facile fractionation of spent coffee grounds into sustainable aviation fuel–relevant streams using methanol and potential endogenous alcohol–glycerol solvent mixtures

Christopher Acquah,[a] Kerby C. Jones,[b] Victor T. Wyatt,[b] Valerie García-Negrón,[b] Emmanuel A. Aboagye,[c] Wo Bin Bae,[a] Ishmaiah E. Small,[a] Jack E. Kleissler,[a] Joseph F. Stanzione III,[a,d] Jun Hee Jang*[a,d]

a. Department of Chemical Engineering, Rowan University, Glassboro, NJ 08028, USA.

b. †Sustainable Biofuels and Co-Products Research Unit, Eastern Regional Research Center, USDA-ARS, Wyndmoor, PA 19038, USA.

c. Department of Chemical and Biological Engineering, Princeton University, Princeton, NJ 08544, USA.

d. Advanced Materials & Manufacturing Institute (AMMI), Rowan University, 201 Mullica Hill Road, Glassboro, New Jersey 08028, USA

† Mention of trade names or commercial products in this publication is solely for providing specific information and does not imply recommendation or endorsement by the U.S. Department of Agriculture. USDA is an equal opportunity provider and employer.

Email: jang@rowan.edu

## Analytical methods

### *Compositional analysis*

Biomass compositional analysis was conducted as described in the standard NREL protocol (NREL-TP-510-42618).[1] Moisture analysis consisted of heating the samples at 105 °C for at least 4 h in a drying convection oven (Fisherbrand Isotemp, Fisher Scientific), followed by placing them in a desiccator for about 1 h, and then weighed at room temperature. For the compositional analysis, 0.30 g of dry biomass solids was used in triplicate for each unique sample condition. Each sample was mixed with 3.0 mL of 72 % w/w sulfuric acid (Fluka) and stirred every 5 min for a total of 1 h in a water bath at 30 °C. Afterwards, the sample solutions were diluted with 84 mL of deionized water, sealed in 100 mL pressure flasks, and set in the autoclave for hydrolysis at 121 °C for about 1.5 h. Samples were then allowed to cool to room temperature and filtered through ceramic crucibles to separate the acid insoluble residue (AIR) from the liquid fractions. The AIR was dried and weighed to determine acid-insoluble lignin (AIL), with ash correction performed according to the NREL protocol. Acid-insoluble lignin (AIL) values were corrected by subtracting the measured lipid content remaining in each fraction. Because SCG contain residual lipids, the measured AIL values were further corrected by subtracting the lipid content remaining in the acid-insoluble residue. To validate this correction approach, dried SCG was first defatted via hexane Soxhlet extraction and subsequently subjected to the same two-stage acid hydrolysis procedure. The AIL value obtained from defatted SCG closely matched the lipid-corrected AIL value (difference within ±3%), confirming that lipid subtraction does not introduce significant bias in lignin quantification.

The recovered solids from the acid-insoluble lignin fractions were weighed. First, they were placed in a drying convection oven at 105 °C for 24 h, then placed in a furnace (Thermo Scientific, Lindberg/Blue M) at 575 °C for 24 h; after cooling to room temperature, the ash content was measured. For the liquid fraction, acid-soluble lignin was determined using a Shimadzu UV-1800 UV/Vis spectrophotometer (Somerset, NJ, USA). The liquid fraction was also analyzed for sugars using a high-performance liquid chromatography (HPLC) 1100 series instrument (Agilent Technologies, Santa Clara, CA, USA) equipped with an Aminex HPX-87P column (Bio-Rad Laboratories, Inc., Hercules, CA, USA). A 10 µL aliquot from each liquid sample was filtered through a 0.20 µm membrane and transferred to 1.5 mL HPLC vials. The HPLC column was set at 80 °C with chromatography-grade water as the mobile phase at a flow rate of 0.6 mL min$^{-1}$, and samples were injected at 5 µL, in duplicate.

***Protein analysis***

Protein analysis was conducted using a Flash EA 1112 Series (Thermo Finnigan) instrument dedicated to nitrogen and protein analysis. Triplicate samples were prepared, placed in tin cups and sealed with tweezers. The reactor operated at 950 °C under flowing oxygen, while the column detector was maintained at 50 °C; helium served as both the carrier and reference gas. Total nitrogen content was measured and converted to protein concentration using a conversion factor of 6.25.

***Lipid (fat) analysis***

For fat content analysis, approximately 0.50 g of sample was placed into ANKOM XT4 filter bags and heat-sealed. The bags were dried at 105 °C for at least 3 h to remove moisture, then cooled in a desiccator. The dried bags were loaded into an ANKOM XT10 extractor (ANKOM Technology, Macedon, NY, USA) and extracted with 350 mL of hexane at 105 °C for 2 h. Lipids were also extracted using a Soxhlet apparatus with hexane, and any residual lipid after hexane extraction was verified using an accelerated solvent extraction method. Combined compositional and lipid analyses indicated that SCG contained approximately 50 wt % carbohydrates, 30 wt % lignin and 8 wt % lipids, based on triplicate measurements.

***Thin-layer chromatography (TLC)***

Separations were performed using Analtech (Newark, DE, USA) Silica Gel G TLC plates (10 cm × 20 cm, 250 µm thick). The development solvent mixture was 80:20:1 hexane:diethyl ether:acetic acid. A 5 % phosphomolybdic acid solution in ethanol was used for visualization, followed by heating. Approximately 10 mg of sample was diluted with 1.0 mL of methylene chloride (dichloromethane); 2 µL of this mixture was spotted onto the TLC plate for analysis.

***Gas chromatography (GC-MS/FID)***

*GC-MS (identification)*

A GC (Agilent Technologies, Model 8890) equipped with a mass-selective detector (Agilent Technologies, Model 5977) and SP-2380 column (30 m × 0.25 mm × 0.20 µm) from Supelco was utilized to analyze the fatty acid methyl esters (FAME) profile of reaction products. The column was initially heated at 50 °C for 1 min and ramped up to 180 °C at a rate of 30 °C $min^{-1}$, then a second ramp to 210 °C was done at a rate of 2 °C $min^{-1}$ which was then held for 5 min. Helium was used as a carrier gas which was set to flow at 1 mL $min^{-1}$ with a split ratio of 5:1. The temperature of the injector and detector were 210 °C and 240 °C, respectively.

*Sample preparation for GC-MS*

For GC-MS analysis, approximately 100 mg of sample was added in 5 mL reaction vials followed by the addition of methyl tert-butyl ether (1 mL) along with 2 % $H_2SO_4$ in methanol (1 mL) and the reaction vials were capped and stirred at 70 °C for 1 h. The reaction mixture was cooled at room temperature, and 1 mL DI water was added to form two layers. The upper organic layer was extracted with hexane twice (2 mL) and washed with water (2 mL) once. The hexane extract containing FAME was dried over anhydrous $Na_2SO_4$ then evaporated to residue using nitrogen. 10 µL of FAME sample was diluted with 1 mL of ethyl acetate before injection for GC-MS analysis.

*GC-FID (quantification)*

A solution was prepared by dissolving 20.0 mg of hexane-soluble oil and 10.0 mg of 1,3,5-tri-tert-butylbenzene (TTB, internal standard) in a 2 mL vial, followed by dilution to 1.00 mL with HPLC-grade methanol. The mixture was vortexed for 30 s, filtered through a 0.20 µm PTFE membrane, and 1 µL was injected.

*Instrument conditions (GC-FID)*

GC–FID analyses were performed on an Agilent 7890B equipped with an HP-5MS column (Agilent 19091S-433, 30 m × 0.25 mm × 0.25 µm). Helium was used as the carrier gas at a constant flow of 0.4588 mL $min^{-1}$ (average linear velocity ~14.4 cm $s^{-1}$; hold-up time ~3.48 min). The inlet was operated in split mode at 280 °C with a split ratio of 100:1, septum purge flow of 3 mL $min^{-1}$, and gas saver flow of 20 mL $min^{-1}$ after 2 min. The oven program was 70 °C (2 min), ramped at 5 °C $min^{-1}$ to 280 °C (2 min), for a total run time of 46 min. The FID was maintained at 300 °C with $H_2$ at 30 mL $min^{-1}$, air at 400 mL $min^{-1}$, and makeup helium at 5 mL $min^{-1}$. Data were collected at 50 Hz with a zero time set at 0 min.

*Calibration and calculation*

20 mg of the commercial FAME standard mixture (TCI, Standard Mixture of Fatty Acid Methyl Esters) and 10 mg of TTB as an internal standard were weighed. The mixture was brought up to 2.00 mL with HPLC-grade methanol, vortexed for 30 s, filtered through a 0.20 µm PTFE membrane and analyzed by GC-FID. These injections were used to determine class- or compound-specific response factors ($RF_i$) for the FAME components relative to TTB. Mass fraction for species i was calculated as: $w_i(\%) = (A_i / A\_TTB) \times (m\_TTB / m\_sample) \times RF_i \times 100$, where $A_i$ and A_TTB are FID peak areas. Totals were reported as the sum of response-factor-corrected species, normalized to 100 %, with GC-MS used to confirm identities.

***HPLC***

Separations were made on a Phenomenex (Torrance, CA) IB-sil cyanopropyl 5 µm (CN) column (250 × 4.6 mm i.d.) with an accompanying guard column (30 × 4.6 mm i.d.) of the same phase and a flow rate of 1.0 mL $min^{-1}$. HPLC was conducted with an Agilent 1100 series liquid chromatograph consisting of vacuum degasser, quaternary pump and autosampler modules. A Polymer Labs ELS1000 evaporative light scattering detector (ELSD) was used for detection. Program control, data acquisition and analysis were carried out using Agilent ChemStation version 9.03.

*Calibration*

Neutral lipid component calibration curves were determined using serial dilutions of Nu Chek Prep TLC (Elysian, MN) standard mixture (18-1A) + oleic acid in hexane. Each level was determined using triplicate injections (2000-100 ng $mL^{-1}$) at 10 µL each.[2]

*Sample preparation for HPLC*

10 mg of samples were diluted with 1.0 mL of hexane, then filtered with a 0.45 µm PTFE filter; 10 µL was injected into the HPLC system for analysis.

HPLC gradient program

| Time (min) | %A | %B |
|---|---|---|
| 0.0 | 100 | 0 |
| 5.0 | 98 | 2 |
| 15.0 | 20 | 80 |
| 17.0 | 20 | 80 |
| 17.1 | 100 | 0 |
| 27.0 | 100 | 0 |

A = hexane + 0.4 % acetic acid    B = methyl tert-butyl ether (MTBE) + 0.4 % acetic acid

Detector parameters

$N_2$ flow = 1.3 SLPM; nebulizer = 45 °C; evaporator = 40 °C

**Table S1.** Comparison of solvent-based extraction/fractionation studies of spent coffee grounds (SCG).

| Study (scope) | Solvent system & key conditions | Main products/streams (key results) | Characterization reported |
|---|---|---|---|
| Bitencourt et al. (2020, J. Supercrit. Fluids) High-pressure oil/extractives fractionation[3] | 333 K; ~40 MPa; 1–2 step extraction Solvents: $scCO_2$, EtOH, $scCO_2$+EtOH (90:10 w/w) | Coffee oil / extractives only Max overall extract yield: 25% (EtOH) TPC: 4.56 mg GAE/g extract (EtOH) | Overall yield + TPC; focus on oil/extractives |
| Araújo et al. (2019, Ind. Crops Prod.) Pressurized fluid oil extraction[4] | Semi-batch extraction using $scCO_2$+EtOH; compared with $scCO_2$ and pressurized EtOH | Coffee oil / extractives | Extraction yield comparisons; oil properties (reported in the study) |
| Al-Hamamre et al. (2012, Fuel) Solvent screening for oil[5] | Conventional solvent extraction (multiple solvents screened) | Best oil yield reported with n-hexane (~15.3% db) Oil used for biodiesel production | Oil yield; fuel/biodiesel properties |
| Somnuk et al. (2017, Agriculture and Natural Resources) Solvent screening/optimization[6] | Solvent extraction (hexane, i-PrOH, EtOH) with process optimization | Max oil yields: 14.7 wt% (hexane), 13.1 wt% (anhydrous ethanol), 11.8 wt% (hydrous ethanol), 7.5 wt% (methanol) | Oil yield + basic quality/composition metrics |
| Efthymiopoulos et al. (2018, Ind. Crops Prod.) Solvent & temperature effects[7] | Soxhlet with wide solvent set; accelerated solvent extraction (ASE) up to ~200 °C | Oil extraction efficiency trends EtOH gave highest oil extraction ratio by ASE (~165 °C) | NMR + titration (FFA); composition trends vs solvent |
| Loyao Jr. et al. (2018, Ind. Crops Prod.) Alternative solvents for oil[8] | Solvent extraction with alternative solvents (e.g., EtOAc, alcohols) Includes washing/re-extraction step | Oil extraction yield depends on solvent & time; washing/re-extraction affects reported 'extract' yields | Oil yield/recovery methodology; oil quality metrics |
| Chemat et al. (2022, OCL) Green solvent vs hexane[9] | Defatting with 2-methyloxolane (2-MeOx) vs n-hexane | Lipid yields: 12.47 ± 0.89% (hexane), 13.67 ± 0.14% (dry 2-MeOx), 15.84 ± 0.96% (water-saturated 2-MeOx) | Oil yield + defatted-biomass considerations |
| Panusa et al. (2013, J. Agric. Food Chem.) Antioxidant extractives[10] | Solid–liquid extraction with water and hydroalcoholic mixtures | Phenolic/caffeine-rich extracts; TPC reported in the range ~6–28 mg GAE/g | UHPLC/compound identification + antioxidant assays |
| Xu et al. (2015, Ind. Crops Prod.) Subcritical water extractives[11] | Subcritical water extraction (pressurized hot water) | Antioxidative phenolic fraction recovered (extractives-focused) | Phenolic content + antioxidant activity |
| Page et al. (2017, Waste Manag.) Crude ethanolic extract[12] | Ethanol extraction of SCG | Ethanolic extract (volatile + functional properties) targeted | Volatile profile + functional properties |

| | | | |
|---|---|---|---|
| Silva et al. (2025, Molecules)<br>Aqueous ultrasonication[13] | Ultrasonication in water (single-step) | Two products: (i) aqueous extract (caffeine ~400 mg/100 g; polyphenols ~800 mg GAE/100 g)<br>(ii) fiber-rich solid (~73 g/100 g dietary fiber) | Bioactive quantification; fiber composition |
| Ravindran et al. (2018, Bioresour. Technol. Rep.)<br>Organosolv pretreatment[14] | Modified organosolv (EtOH–$H_2O$) with acid catalyst (e.g., 1.5% $H_2SO_4$)<br>~51 °C, 45 min (reported) | Polyphenols (11.2 mg GAE/g), partial lignin removal (24.4%), sugars (29.05 mg/g) for downstream bioconversion | XRD; FT-IR; DSC (reported) |
| Corrado et al. (2024, Sep. Purif. Technol.)<br>Cascade biorefinery (DES)[15] | Multi-step: delipidization → hydroalcoholic extraction → DES (ChCl:lactic acid) → saccharification → fermentation | Recovered: oil 13.0 g/100 g; phenols 9.6 g/100 g; lignin 6.2 g/100 g; sugars 11.6 g/100 g (reported)<br>Overall recovered compounds ~45 wt% | Antioxidant assays + biomass conversion metrics |
| Pérez-Merchán et al. (2025, J. Cleaner Prod.)<br>Organosolv fractionation[16] | Organosolv fractionation of SCG (paper-industry style) | Hemicellulosic liquor with up to 25 wt% sugars (galactose/mannose)<br>HMF yield up to 90% in 15 min (from hemicellulose liquor) | XRD + FT-IR of cellulose/lignin fractions |
| Kwon et al. (2013, Bioresour. Technol.)<br>Biodiesel + bioethanol[17] | Sequential processing (lipid extraction + non-catalytic transesterification; separate saccharification/fermentation) | Bioethanol yield 0.46 g/g (based on consumed sugar) Biodiesel yield 97.5 ± 0.5% (from extracted lipids) | Biofuel yields; basic process performance |
| Rocha et al. (2014, Bioresour. Technol.)<br>Ultrasound-assisted fuels[18] | Ultrasound-assisted extraction + conversion routes | Oil extraction yield ~12% (reported) and biodiesel yields up to ~97% FAME; ethanol production evaluated | Biofuel yields/FA profile (reported) |
| Battista et al. (2021, Bioresour. Technol.)<br>Integrated biorefinery[19] | Integrated route combining lipid conversion + carbohydrate valorization (uses glycerol in pretreatment/processing) | Reported biodiesel performance (~86% w/w) and fermentable sugar release (~40–50% w/w) | Process performance metrics |
| This work<br>Alcohol-solvolysis whole-biomass fractionation | Alcohol solvolysis (MeOH; MeOH/glycerol; EtOH/glycerol) 180–200 °C; followed by staged separations (hexane + water) | Four separable streams: carbohydrate-rich solid + lipid-rich oil + water-extract solubles + lignin-rich oil<br>Combined SAF-convertible fractions: 61–66 wt%<br>Autogenous pressure: 15.6 bar (EG_200; 59% lower than MeOH)<br>MSP: $1.43/kg (EG_200; ~30% lower than MeOH case) | Compositional analysis; GC-FID/MS; HPLC lipid class; FT-IR; NMR; GPC (all streams) |

**Calculation equations**

$$Delignification\ (wt\%) = \left(1 - \frac{mass_{lignin} in\ solid\ residue}{mass_{lignin} in\ dried\ SCG}\right) \times 100\#(S1)$$

$$Delipidification\ (wt\%) = \left(1 - \frac{mass_{lipid} in\ solid\ residue}{mass_{lipid} in\ dried\ SCG}\right) \times 100\ \#(S2)$$

$$Glucan\ retention\ (wt\%) = \left(\frac{mass_{glucan} in\ solid\ residue}{mass_{glucan} in\ dried\ SCG}\right) \times 100\ \#(S3)$$

$$Mannan\ retention\ (wt\%) = \left(\frac{mass_{mannan} in\ solid\ residue}{mass_{mannan} in\ dried\ SCG}\right) \times 100\#(S4)$$

$$Solid\ Recovery\ (wt\%)\ = \left(\frac{mass_{solid\ residue}}{initial\ dried\ SCG}\right) \times 100\#(S5)$$

$$Hexane - extracted\ oil\ yield\ (wt\%)\ = \left(\frac{mass_{hexane\ -\ extracted\ oil}}{initial\ dried\ SCG}\right) \times 100\#(S6)$$

$$Solvolysis\ oil\ yield\ (wt\%) = \left(\frac{mass\ of\ solvolysis\ oil}{initial\ dried\ SCG}\right) \times 100\#(S7)$$

**Table S2**. Compositional analysis of brewed SCG and post-solvolysis solid samples in methanol and methanol/ethanol/glycerol mixtures.

| wt.% | Brewed SCG | MS_180 | MS_200 | MS_220 | MG_200 | EG_200 | ES_200 |
|---|---|---|---|---|---|---|---|
| Glucan | 8.4 | 12.3 | 13.0 | 15.0 | 13.8 | 13.3 | 12.1 |
| Galactan | 10.2 | 13.9 | 12.6 | 13.0 | 9.8 | 9.9 | 13.2 |
| Mannan | 30.7 | 45.0 | 38.5 | 35.9 | 45.0 | 42.1 | 40.0 |
| Total lignin | 30.6 | 21.8 | 22.8 | 24.4 | 22.3 | 18.0 | 24.8 |
| AI Lignin | 28.6 | 20.6 | 21.7 | 23.3 | 21.5 | 17.2 | 23.2 |
| AS lignin | 2.0 | 1.2 | 1.1 | 1.1 | 0.8 | 0.8 | 1.6 |
| Glycerides | 8.0 | 0.5 | 0.7 | 0.7 | 0.7 | 1.0 | 0.5 |
| Protein | 12.1 | 8.2 | 7.6 | 15.4 | 8.6 | 7.4 | 8.2 |
| Ash | 0.1 | 0.6 | 1.7 | 1.1 | 1.0 | 0.4 | 0.4 |
| Total | 100.0 | 102.3 | 96.9 | 105.4 | 101.1 | 92.2 | 99.2 |

**Table S3.** Dry-basis compositional comparison of the brewed spent coffee grounds (SCG) used in this work with representative literature reports. Values are reported as wt% on a dry SCG basis. A dash (–) indicates the component was not reported or not explicitly separated in the cited reference. Reported differences across studies can arise from SCG origin and processing (e.g., brewing conditions, defatting/extractive removal efficiency) and analytical protocol details. Values reported as ranges (e.g., Johnson et al., 2022) reflect literature compilations across multiple primary sources rather than a single SCG sample.

| Component wt% dry basis | This work (Brewed SCG) | Ribeiro et al. 2023[20] | Caetano et al. 2014[21] | Lee et al. 2019[22] | Johnson et al. 2022[23] |
|---|---|---|---|---|---|
| Glucan/cellulose | 8.4 | 9.55 | 15.3 | 9 | 13.8–14.8 |
| Galactan | 10.2 | - | - | - | - |

| | | | | | |
|---|---|---|---|---|---|
| Mannan | 30.7 | - | - | - | - |
| Acid-insoluble lignin (AIL) | 28.6 | 28.59 | 30.9 | - | 28.2–31.9 |
| Acid-soluble lignin (ASL) | 2 | 2.14 | 1.6 | - | 1.7–2.82 |
| Total lignin (AIL+ASL) | 30.6 | 30.73 | 32.5 | 28.2 | 32.5–33.6 |
| Lipids / glycerides | 8 | - | 6 | 14.9 | 8–20 |
| Protein | 12.1 | - | 12.3 | - | - |
| Ash | 0.1 | 1.66 | 1.65 | 1.8 | 1.7–2.9 |

**Table S4.** Stream-by-stream characterization summary and where key values are reported.

| **Stream / fraction** | **Where data are reported** | **Analytical methods used** | **Key quantitative results (yield/composition)** |
|---|---|---|---|
| Carbohydrate-rich solid residue | Solid composition: **Figure 2A**, **Table S2**<br><br>Fractionation metrics **Figures 2C** and **4A**<br><br>Stream yields, mass balance: **Figures 2B** and **4B** | NREL compositional analysis method<br><br>Mass measurement | Solid yield (wt% dry SCG): 67.8 (MS_180), 61.1 (MS_200), 53.8 (MS_220), 64.7 (ES_200), 54.7 (MG_200), 55.2 (EG_200)<br><br>Retention (solid phase): glucan 96.3–99.5%; mannan 62.9–99.3%; galactan 68.9–92.6% (methanol series). EG_200: glucan 88%, mannan 76%, galactan 54%<br><br>Delipidification 94.4–95.7% (methanol series); EG_200 92.9%.<br><br>Delignification 51.6–57.1% (methanol series); EG_200 67.5% |
| Hexane-extracted oil (lipid-rich fraction) | Oil yields: **Figures 2B** and **4B**<br><br>HPLC/GC-MS/FID and GPC: **Figure 3**<br><br>NMR and FT-IR: **Figures S2** and **S3**. | HPLC for neutral-lipid class analysis<br><br>GC-FID and GC-MS for FAME analysis<br><br>FT-IR; $^{1}H$/2D-HSQC NMR; GPC | Yield (wt% dry SCG): 12.5 (MS_180), 15.3 (MS_200), 16.7 (MS_220), 11.7 (ES_200), 16.7 (MG_200), 15.1 (EG_200)<br><br>Lipid derivatives: ~7–10 wt% on a dry-SCG basis; lipids are ~50–60 wt% of the hexane extract (remainder is co-extracted low-MW aromatics)<br><br>Major FAME species include methyl palmitate and methyl linoleate; higher temperature increases ester-dominated profile |
| Water-extracted soluble fraction | Water-extracted solids and glycerol (estimated) yields: **Figure 2B**<br><br>Glycerol identification: **Figure S1** | Gravimetric recovery of water-extracted solids after drying<br><br>$^{1}H$ NMR for glycerol identification | Water-extracted solids yield (methanol series): 5.0 (MS_180), 5.3 (MS_200), 7.1 (MS_220) wt% dry SCG<br><br>Glycerol estimated from lipid conversion accounting: 0.3–0.8 wt% dry SCG; glycerol directly identified in aqueous extract |

| Stream / fraction | Where data are reported | Analytical methods used | Key quantitative results (yield/composition) |
|---|---|---|---|
| Undissolved lignin-rich oil fraction | Oil yields: **Figures 2B** and **4B**<br><br>NMR, GPC and GC-FID: **Figures S4–S6** | GPC after acetylation<br><br>$^1$H and 2D HSQC NMR for lignin identification<br><br>GC-FID for low MW lignin identification | Yield (wt% dry SCG): 13.4 (MS_180), 17.1 (MS_200), 19.5 (MS_220), 22.6 (ES_200), 27.2 (MG_200), 26.8 (EG_200)<br><br>MW distribution: dominant 270–300 Da peak with oligomers/polymers up to ~16 kDa<br><br>SAF-convertible fraction (110–450 Da): 47–52 wt% of lignin-rich oil |

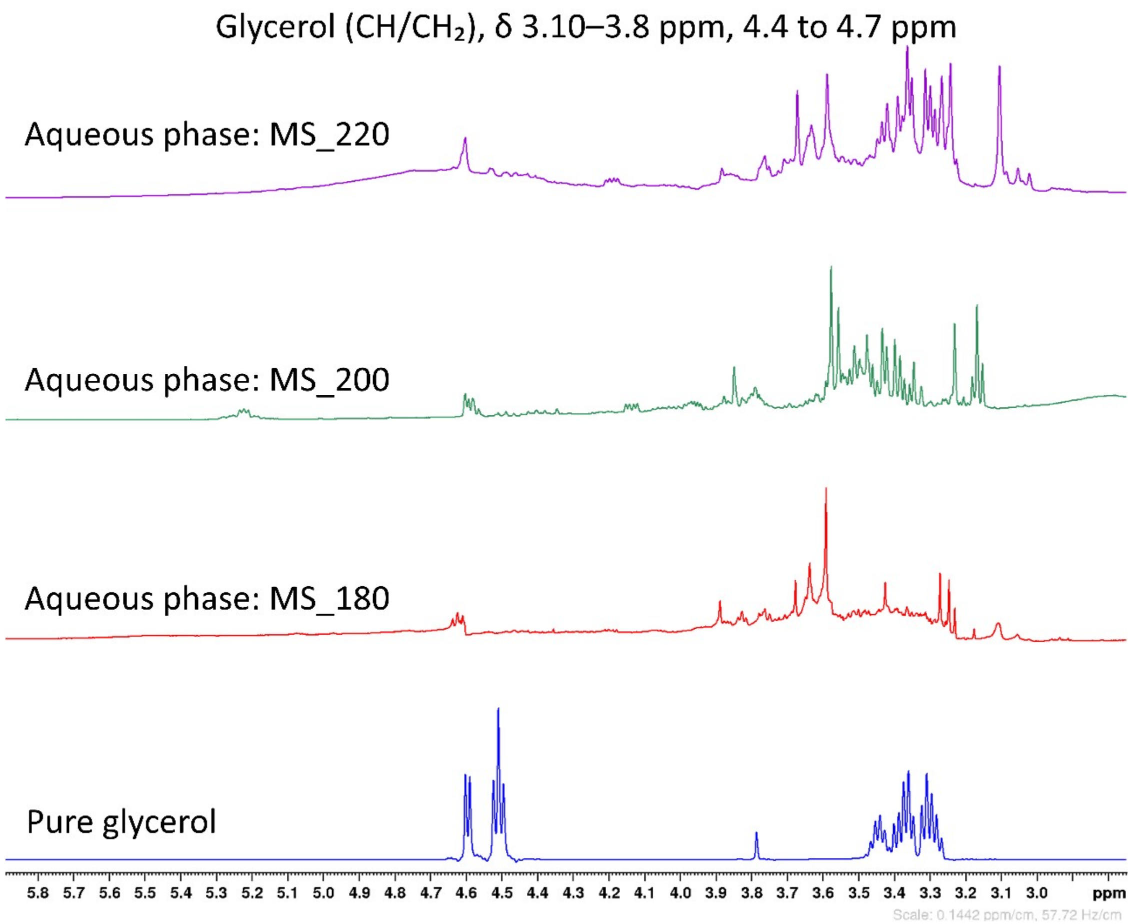


**Figure S1.** $^1$H NMR spectra (DMSO-$d_6$) of the water-extracted (aqueous) fraction obtained after sequential hexane/water extraction of the solvolysis oil for MS_180, MS_200, and MS_220, shown together with a neat glycerol reference (bottom). Spectra are offset for clarity. The aqueous extracts display the characteristic glycerol $CH/CH_2$ resonance envelope at δ ~3.10–3.85 ppm, together with the additional glycerol signal region at δ ~4.4–4.7 ppm, which aligns with the neat glycerol reference. This confirms that glycerol is present in the aqueous extract and supports the interpretation of in-situ glycerol formation during solvolysis (from glyceride transesterification/hydrolysis).

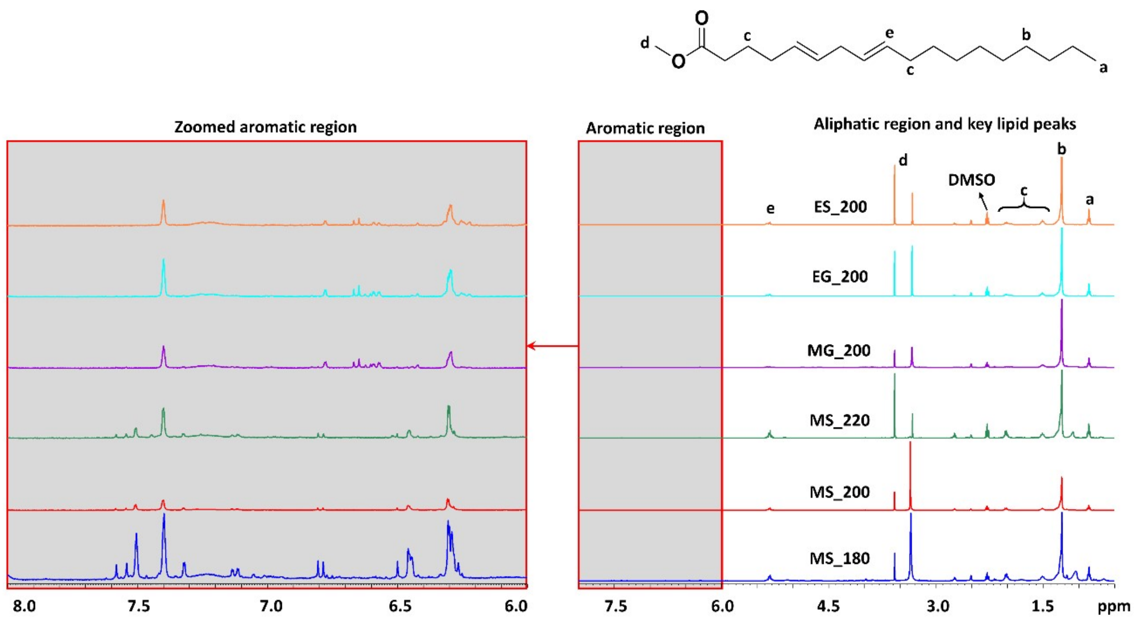


**Figure S2**. $^{1}H$ NMR spectra (DMSO-$d_6$) of the hexane-extracted oil obtained from solvolysis under different solvent conditions (MS_180, MS_200, MS_220, MG_200, EG_200, and ES_200). Spectra are stacked and vertically offset for clarity. The right panel shows the full spectral window highlighting the aliphatic region and key lipid resonances, while the left panel provides a zoomed view of the aromatic region (δ 8.0–6.0 ppm). A representative fatty acid methyl ester (FAME) structure is shown above the spectra with labeled protons (a–e) to guide peak assignment. Major resonances include terminal $-CH_3$ (δ 0.8–1.0), bulk aliphatic $-(CH_2)n-$ (δ 1.1–1.5), methylene groups adjacent to unsaturation or ester functionalities (δ 1.6–2.4), the $-OCH_3$ (δ 3.6–3.7), and olefinic protons (δ 5.2–5.4). The presence and relative intensity of these lipid-associated features across solvent conditions indicate the recovery of lipid-derived species in the hexane fraction. Signals observed in the aromatic region (δ 8.0–6.0 ppm) further suggest co-extraction of aromatic compounds alongside lipid derivatives. However, the relative intensity of aromatic signals is substantially lower than that of the aliphatic lipid-associated resonances, indicating that the hexane fraction is predominantly lipid-derived.

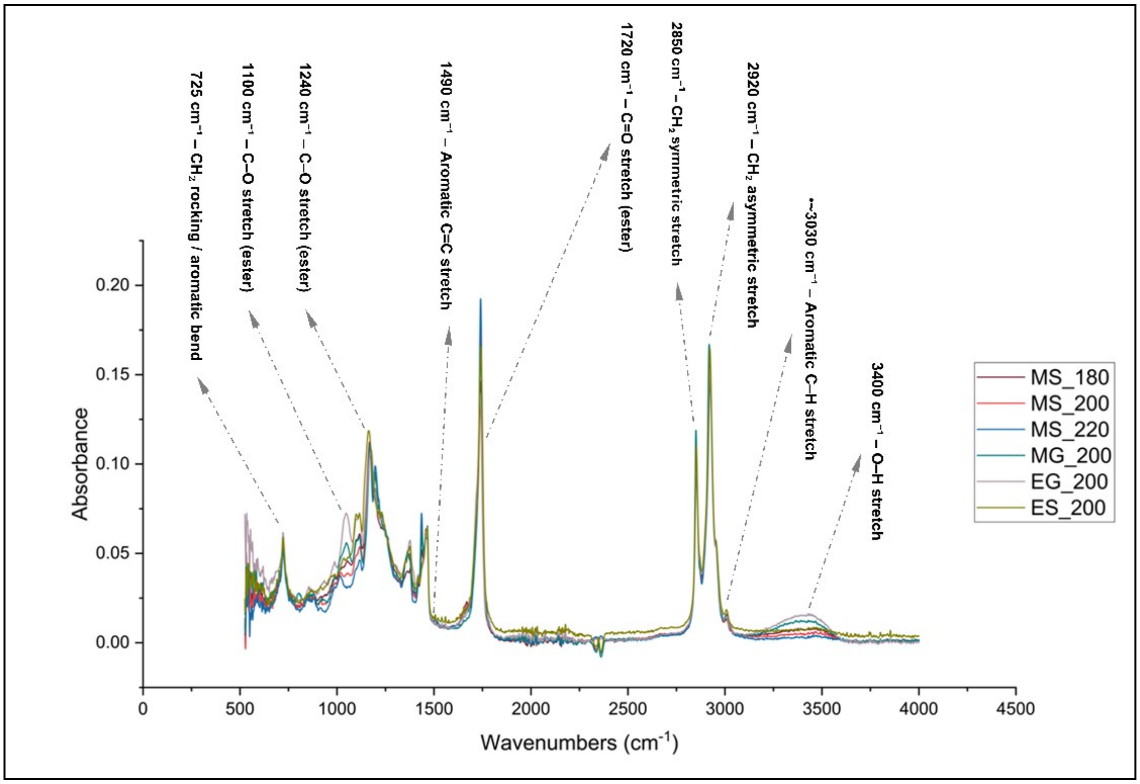


**Figure S3**. FT-IR spectra of the hexane-extracted oils from MS_180, MS_200, MS_220, MG_200, EG_200, and ES_200 (overlaid for comparison). The spectra show the expected ester/lipid-associated bands, including the ester C=O stretch (~1720 $cm^{-1}$) and C–O stretching bands (~1240 and ~1100 $cm^{-1}$), together with strong aliphatic $–CH_2–$ stretches (~2920 and ~2850 $cm^{-1}$) and $–CH_2$ rocking (~725 $cm^{-1}$), confirming the presence of long-chain lipid-derived structures in the hexane fractions. Bands associated with aromatic structures (e.g., aromatic C=C stretching near ~1490 $cm^{-1}$ and aromatic C–H stretching near ~3030 $cm^{-1}$) are also observed, consistent with the co-extraction of aromatic fragments. A broad O–H stretch (~3400 $cm^{-1}$) is present to varying extents, indicating hydroxyl-containing components (e.g., residual acids/alcohols/phenolics) in these oils. Overall, the FT-IR results corroborate the NMR/GC-based interpretation that the hexane-extracted oils contain lipid-derived ester functionalities with contributions from aromatic species.

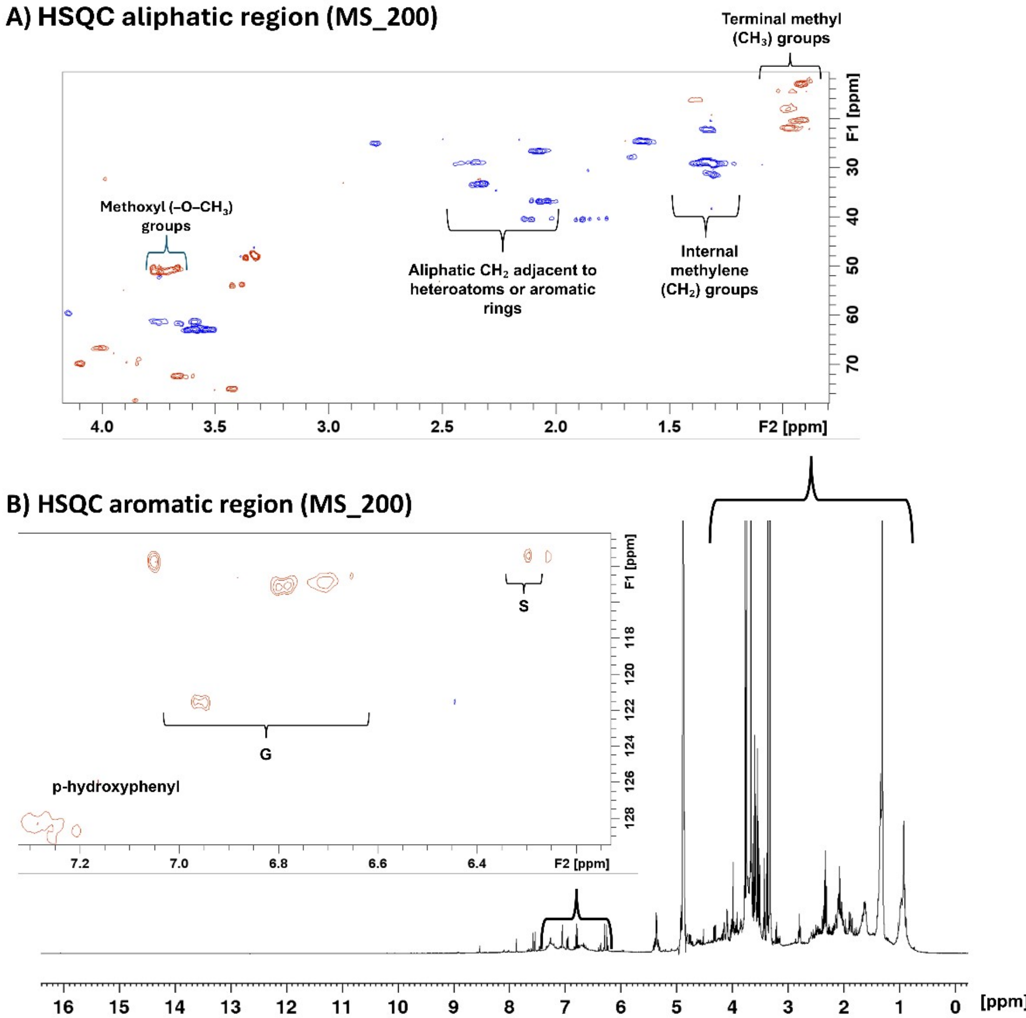


**Figure S4.** $^{1}H$–$^{13}C$ HSQC NMR of the undissolved lignin-rich oil (representative sample: MS_200) acquired in DMSO-$d_6$, presented as **(A)** an aliphatic region and **(B)** an aromatic region. The spectra are annotated to aid interpretation. In the aliphatic region (A), prominent correlations include methoxy (–$OCH_3$) signals at δC/δH ~55/3.7 ppm, along with multiple aliphatic $CH_2$/$CH_3$ correlations attributable to lignin side chains and substituted alkyl environments (including internal methylene and terminal methyl regions). In the aromatic region (B), cross-peaks are observed in chemical-shift ranges consistent with lignin aromatic substructures, including guaiacyl (G)-type signals, syringyl (S)-type signals, and p-hydroxyphenyl-type signals (as labeled). The accompanying $^{1}H$ NMR trace (bottom) provides a 1D view with the aromatic window highlighted. Together, these HSQC features confirm that the undissolved oil is lignin-derived and contains the expected lignin-aromatic motifs, supporting its assignment as a lignin-rich oil fraction.[24, 25]

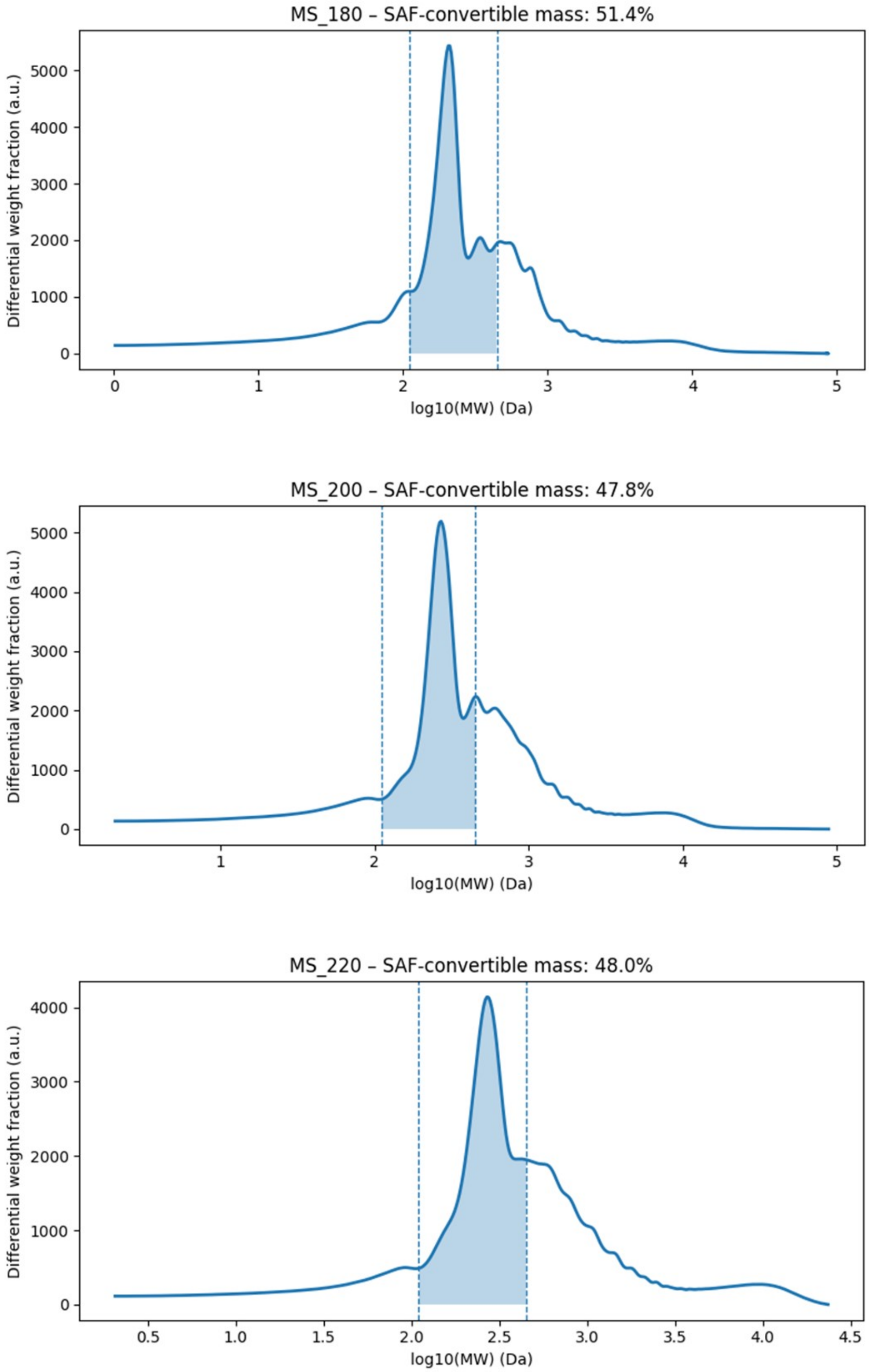


**Figure S5**. GPC-derived molecular-weight distributions of the lignin-rich oils obtained from the methanol temperature series (MS_180, MS_200, and MS_220), plotted as differential weight fraction versus log10(MW). The dashed vertical lines mark the approximate monomer–dimer molecular-weight window (110–450 Da) used here as an operational definition for a readily upgradable ("SAF-convertible") low-MW fraction, and the shaded area represents the integrated mass fraction within this window. The calculated low-MW ("SAF-convertible") fractions are 51.4% (MS_180), 47.8% (MS_200), and 48.0% (MS_220). These distributions indicate that a substantial portion of each lignin-rich oil lies in the lower-MW range, consistent with the presence of depolymerized/aromatic fragments that can be targeted for catalytic upgrading, while the remaining higher-MW tail corresponds to larger oligomeric material.

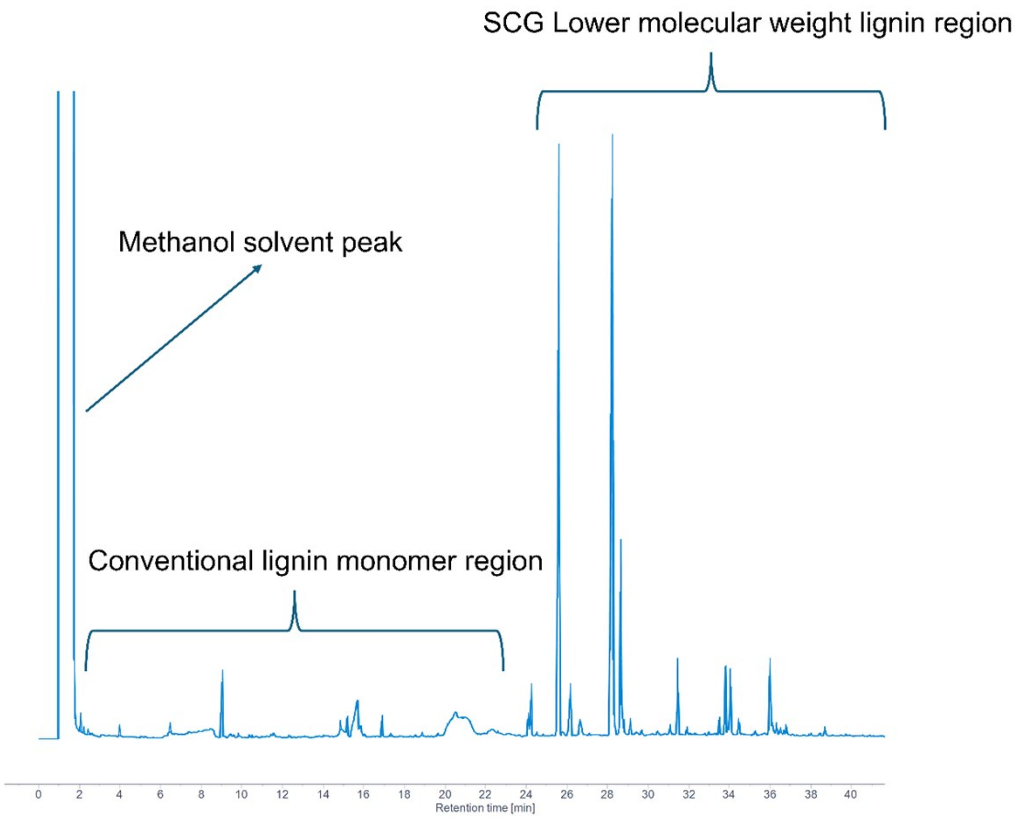


**Figure S6**: GC-FID chromatogram of undissolved lignin oil (representative sample). Only minor GC-amenable peaks are observed; the dominant lignin fraction is higher-molecular-weight material (see **Figure S5**) that is not expected to be readily detected by GC-FID without derivatization.

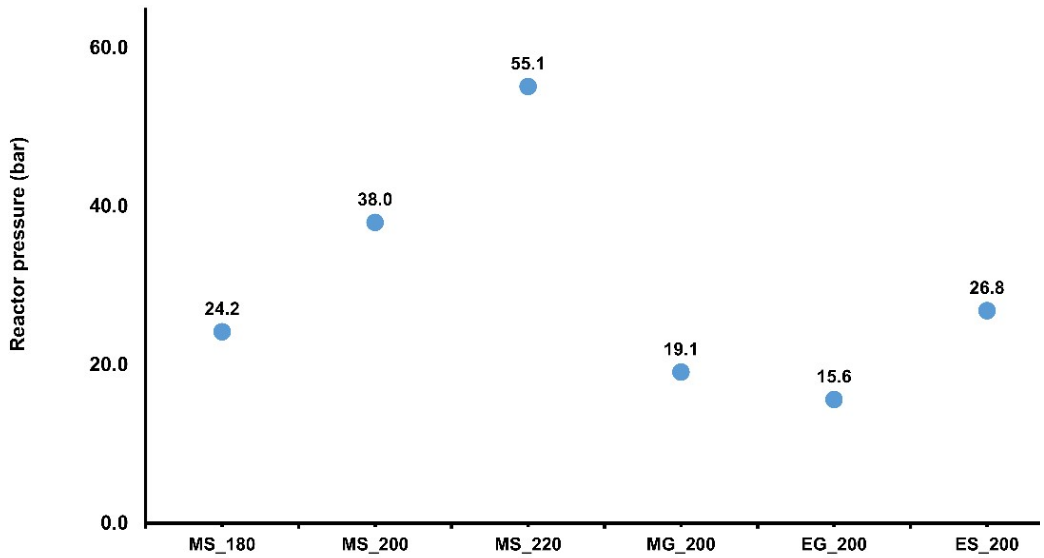


**Figure S7.** Autogenous reactor pressure measured for each solvolysis condition (MS_180, MS_200, MS_220, MG_200, EG_200, ES_200). This figure highlights the operational impact of solvent selection: replacing methanol with ethanol reduces autogenous pressure at 200 °C, and incorporating glycerol as a co-solvent further lowers pressure because of its low volatility, supporting reduced pressure burden while maintaining fractionation performance.

**Process description and techno-economic analysis**

An integrated solvolysis-based biorefinery was developed assuming an nth-plant design with a basis of 2000 dry metric tons of feedstock per day, consistent with previously published work for lignocellulosic biorefineries.[26-30] **Figure 1B** provides a detailed overview of the developed process. In brief, SCG flows to solvolysis reactor, where the reaction takes place at 200°C for 3 h (SOLV area). The reaction product (solvolysis mixture) is separated into three streams: carbohydrate-rich solid stream, crude solvolysis oil stream, and a wastewater stream in the SSEP area. The carbohydrate stream is routed to hydrolysis to produce sugars which are fermented to fuel-grade ethanol via a process consistent with that of Humbird et al.[28] The crude solvolysis oil stream is subjected to distillation for solvent recovery in the SREC area, while the resulting solvent-free solvolysis oil stream is routed for hexane extraction and hydrotreating in the OREC area to produce SAF-intermediate oil (SIO). The resulting wastewater from the ethanol production (ESEP area), solvolysis solvent recovery, and OREC area is routed to wastewater treatment (WWT area) to produce biogas. Higher molecular weight lignin (HMW-lignin) from the OREC area, generated biogas, and unconverted carbohydrate residue from ethanol production are sent to a combined heat and power to generate energy for biorefinery utilities. Aspen Plus v14 was used to simulate the SOLV, SSEP, SREC, and OREC areas shown in **Figure 1B**, while data for the remaining areas (FERM, ESEP, WWT, and CHP) were obtained from reference reports.[26, 28]

Three solvent cases were considered: MS_200 (methanol only), MG_200 (methanol:glycerol 1:1), and EG_200 (ethanol:glycerol 1:1). In the MS_200 case, pure methanol was used for SCG solvolysis in the solvolysis reactor as demonstrated through experimental data. This necessitated the purchase of make-up solvent due to unrecovered methanol at the solvolysis solvent recovery stage and the consumption of methanol to form FAME. In the MG_200, part of the glycerol produced from the SIO recovery stage was diverted together with pure methanol for solvolysis. This approach reduces the amount of make-up methanol needed. In the EG_200 case, solvent for solvolysis was sourced internally from the process: ethanol from fuel-grade ethanol production and glycerol from SIO recovery. For glycerol-containing cases, glycerol is treated as internally generated and recovered for recycle (i.e., no external glycerol purchase is assumed), and the added recovery/recycle handling is captured through the modeled separation duties and operating costs summarized in Table S5.

From the mass and energy balance, TEA was performed to determine the minimum selling price of the SIO (defined as the combined hexane-extracted oil and SAF-range fraction of the undissolved lignin-rich oil). The total capital investment was estimated based on the capital cost of equipment. The operating cost (fixed and variable) was calculated based on material usage and utility requirements. Total costs were offset with revenue from co-products (ethanol and surplus electricity). Finally, the net present value (NPV) methodology was used where we fixed the NPV value to zero and solved a discounted cash flow rate of return at a fixed internal rate of return (20%) and a 30-year plant life to determine the MSP.

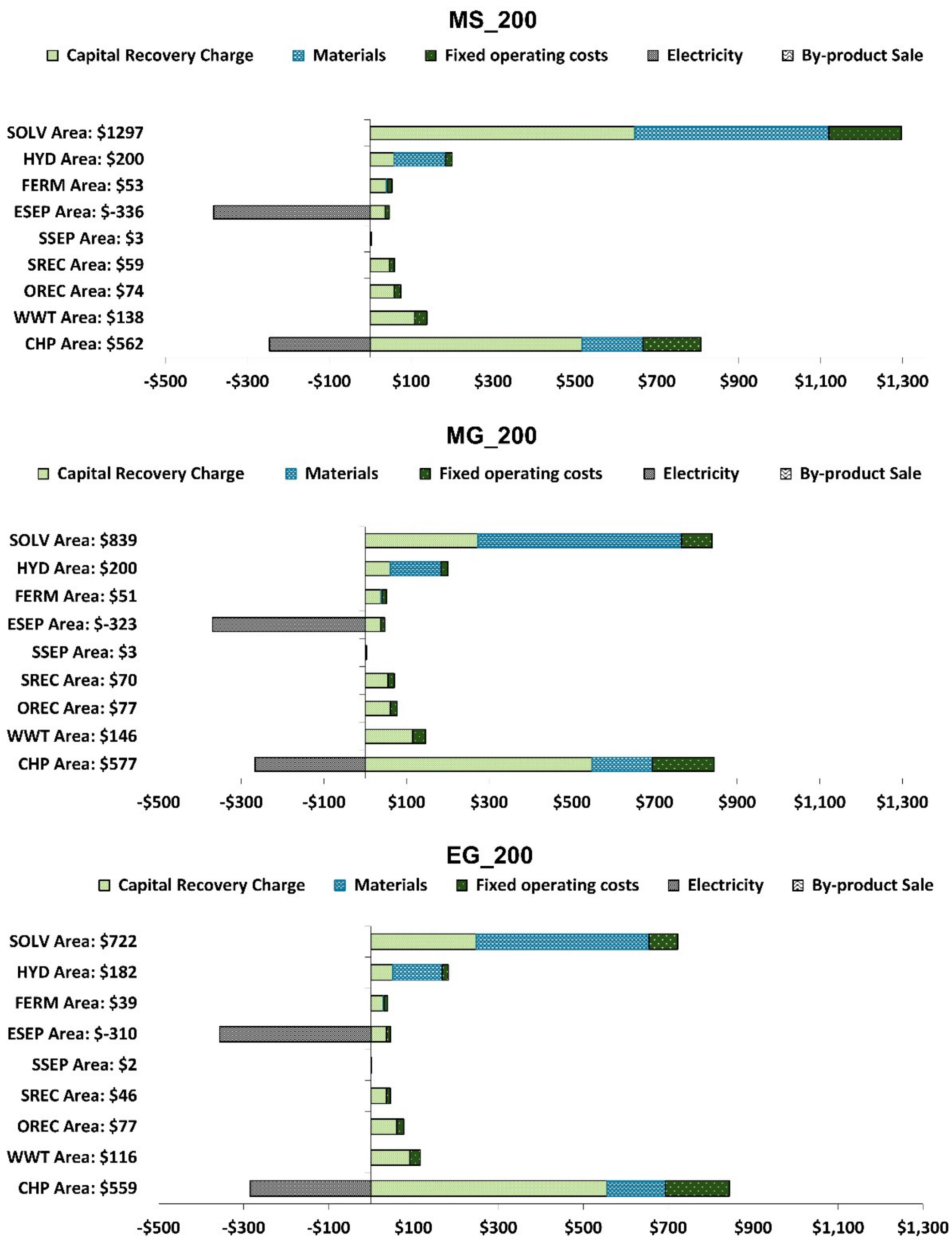


**Figure S8.** Cost breakdown by process area for MS_200 (top), MG_200 (middle), and EG_200 (bottom) solvent systems with minimum selling prices of $2050/tonne ($2.05/kg), $1640/tonne ($1.64/kg), and $1430 /tonne ($1.43/kg) SAF-intermediate oil respectively. Horizontal bars show capital recovery charge (CRC), materials cost (MC), fixed operating costs (FC), electricity (EL), and By-product sale credits. Numbers at left indicate each area's net contribution (per metric ton of SAF-intermediate oil). SOLV and CHP dominate costs, while ESEP appears to have a negative contribution due to ethanol co-product revenue; electricity export credits further reduce MSP. Process areas: SOLV (solvolysis), SSEP (solids separation), HYD (hydrolysis), FERM (fermentation), ESEP (ethanol separation), SREC (solvent recovery), OREC (oil recovery), WWT (wastewater treatment), CHP (combined heat and power).

**Table S5.** Capital and operating expenditure summary (2023 dollar($) value)

**MS_200 (Base Case)**

| | |
|---|---|
| Capital Costs | |
| Solvolysis(SOLV) | $227,584,887 |
| Hydrolysis (HYD) & Enzyme Production | $20,445,467 |
| Fermentation (FERM) | $14,097,368 |
| Ethanol Separation & Storage (ESEP) | $12,883,380 |
| Wastewater Treatment (WWT) | $38,231,440 |
| Combined Heat and power generation (CHP) | $182,239,636 |
| Solvolysis Separation (SSEP) | $704,800 |
| Solvolysis Solvent Recovery (SREC) | $16,371,594 |
| SAF Intermediate Oil Recovery (OREC) | $20,532,608 |

| Manufacturing Costs ($/yr) | |
|---|---|
| Methanol makeup | $13,499,655 |
| Fixed cost | $68,107,730 |
| Feedstock cost + Drying | $51,121,650 |
| Other raw materials | $13,132,291 |

**MG_200**

| | |
|---|---|
| Capital Costs | |
| Solvolysis(SOLV) | $91,129,277 |
| Hydrolysis (HYD) & Enzyme Production | $20,420,219 |
| Fermentation (FERM) | $12,789,559 |
| Ethanol Separation & Storage (ESEP) | $12,350,438 |
| Wastewater Treatment (WWT) | $38,438,235 |
| Combined Heat and Power Generation (CHP) | $183,697,730 |
| Solvolysis Separation (SSEP) | $704,800 |
| Solvolysis Solvent Recovery (SREC) | $18,512,587 |
| SAF Intermediate Oil Recovery (OREC) | $20,304,763 |

| Manufacturing Costs ($/yr) | |
|---|---|
| Methanol makeup | $8,499,655 |
| Fixed cost | $50,892,891 |
| Feedstock cost + Drying | $51,121,650 |
| Other raw materials | $36,404,133 |

**EG_200**

| | |
|---|---|
| Capital Costs | |
| Solvolysis(SOLV) | $82,729,078 |
| Hydrolysis (HYD) & Enzyme Production | $17,124,025 |
| Fermentation (FERM) | $9,757,076 |
| Ethanol Separation & Storage (ESEP) | $12,090,102 |
| Wastewater Treatment (WWT) | $30,525,535 |
| Combined Heat and Power Generation (CHP) | $185,832,486 |
| Solvolysis Separation (SSEP) | $407,800 |
| Solvolysis Solvent Recovery (SREC) | $11,985,256 |
| SAF Intermediate Oil Recovery (OREC) | $20,244,073 |

| Manufacturing Costs ($/yr) | |
|---|---|
| Ethanol makeup (from product recirculation) | $9,499,655 |
| Fixed cost | $47,360,048 |
| Feedstock cost + Drying | $51,121,650 |
| Other raw materials | $13,132,291 |

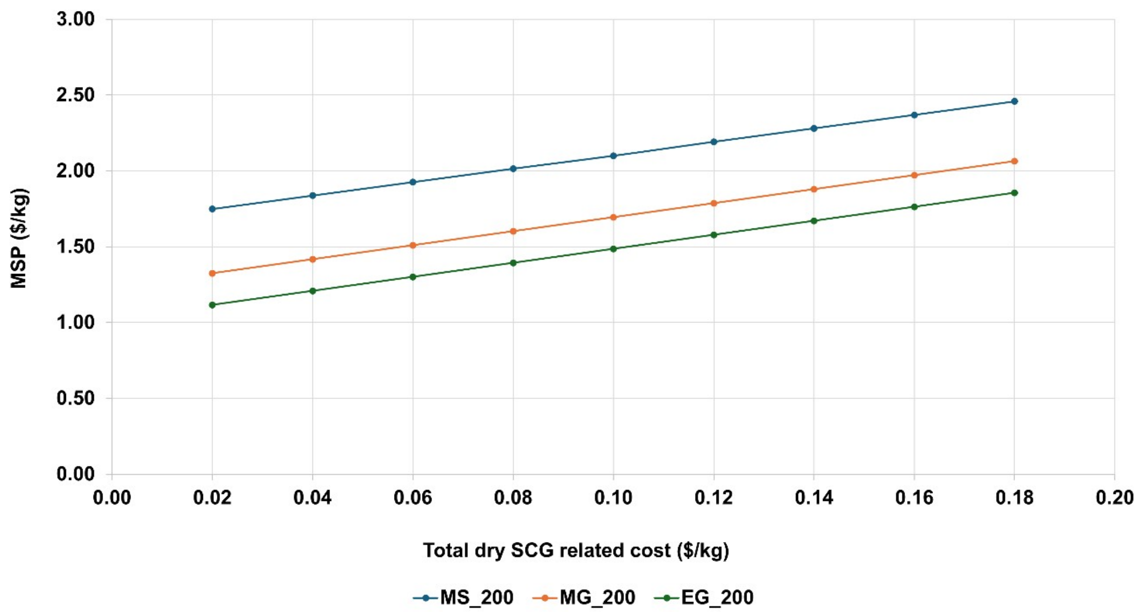


**Figure S9.** Sensitivity of the minimum selling price (MSP) of the SAF-intermediate oil to the total dry SCG-related cost for MS_200, MG_200, and EG_200. The total dry SCG-related cost is defined as the sum of the "Feedstock cost + Drying" and the assumed plant-gate SCG purchase price. The analysis illustrates the impact of variations in feedstock procurement and conditioning costs on the projected MSP.

**References**


1. National Renewable Energy Laboratory (NREL), *Determination of Structural Carbohydrates and Lignin in Biomass: Laboratory Analytical Procedure (LAP)*, https://docs.nrel.gov/docs/gen/fy13/42618.pdf.
2. T. A. Foglia and K. C. Jones, *Journal of Liquid Chromatography & Related Technologies*, 2006, **20**, 1829-1838.
3. R. G. Bitencourt, F. M. P. A. Mello, F. A. Cabral and A. J. A. Meirelles, *The Journal of Supercritical Fluids*, 2020, **157**.
4. M. N. Araújo, A. Q. P. L. Azevedo, F. Hamerski, F. A. P. Voll and M. L. Corazza, *Industrial Crops and Products*, 2019, **141**.
5. Z. Al-Hamamre, S. Foerster, F. Hartmann, M. Kröger and M. Kaltschmitt, *Fuel*, 2012, **96**, 70-76.
6. K. Somnuk, P. Eawlex and G. Prateepchaikul, *Agriculture and Natural Resources*, 2017, **51**, 181-189.
7. I. Efthymiopoulos, P. Hellier, N. Ladommatos, A. Russo-Profili, A. Eveleigh, A. Aliev, A. Kay and B. Mills-Lamptey, *Industrial Crops and Products*, 2018, **119**, 49-56.
8. A. S. Loyao, S. L. G. Villasica, P. L. L. Dela Peña and A. W. Go, *Industrial Crops and Products*, 2018, **119**, 152-161.
9. A. Chemat, H. K. Ravi, A. C. Hostequin, H. Burney, V. Tomao and A.-S. Fabiano-Tixier, *Ocl*, 2022, **29**.
10. A. Panusa, A. Zuorro, R. Lavecchia, G. Marrosu and R. Petrucci, *J Agric Food Chem*, 2013, **61**, 4162-4168.
11. H. Xu, W. Wang, X. Liu, F. Yuan and Y. Gao, *Industrial Crops and Products*, 2015, **76**, 946-954.
12. J. C. Page, N. P. Arruda and S. P. Freitas, *Waste Manag*, 2017, **69**, 463-469.
13. J. Silva, M. T. P. Paiva, H. F. Fuzinato, N. Silvestre, M. T. Benassi and S. Mali, *Molecules*, 2025, **30**.
14. R. Ravindran, C. Desmond, S. Jaiswal and A. K. Jaiswal, *Bioresource Technology Reports*, 2018, **3**, 7-14.
15. I. Corrado, R. Argenziano, E. Borselleca, F. Moccia, L. Panzella and C. Pezzella, *Separation and Purification Technology*, 2024, **334**.
16. A. M. Pérez-Merchán, R. Moreno-Tost, I. Malpartida-García, C. García-Sancho, J. M. Mérida-Robles and P. Maireles-Torres, *Journal of Cleaner Production*, 2025, **528**.
17. E. E. Kwon, H. Yi and Y. J. Jeon, *Bioresour Technol*, 2013, **136**, 475-480.
18. M. V. Rocha, L. J. de Matos, L. P. Lima, P. M. Figueiredo, I. L. Lucena, F. A. Fernandes and L. R. Goncalves, *Bioresour Technol*, 2014, **167**, 343-348.
19. F. Battista, L. Zuliani, F. Rizzioli, S. Fusco and D. Bolzonella, *Bioresour Technol*, 2021, **342**, 125952.
20. G. M. Ribeiro, P. L. Martins, A. C. Oliveira, F. Carvalheiro, R. Fragoso and L. C. Duarte, *Energies*, 2023, **16**.
21. N. S. Caetano, V. F. M. Silva, A. C. Melo, A. A. Martins and T. M. Mata, *Clean Technologies and Environmental Policy*, 2014, **16**, 1423-1430.
22. M. Lee, M. Yang, S. Choi, J. Shin, C. Park, S.-K. Cho and Y. M. Kim, *Energies*, 2019, **12**.
23. K. Johnson, Y. Liu and M. Lu, *Frontiers in Chemical Engineering*, 2022, **4**.
24. R. Samuel, M. Foston, N. Jaing, S. Cao, L. Allison, M. Studer, C. Wyman and A. J. Ragauskas, *Fuel*, 2011, **90**, 2836-2842.
25. E. Sheridan, S. Filonenko, A. Volikov, J. A. Sirviö and M. Antonietti, *Green Chemistry*, 2024, **26**, 2967-2984.
26. A. W. Bartling, M. L. Stone, R. J. Hanes, A. Bhatt, Y. Zhang, M. J. Biddy, R. Davis, J. S. Kruger, N. E. Thornburg, J. S. Luterbacher, R. Rinaldi, J. S. M. Samec, B. F. Sels, Y. Roman-Leshkov and G. T. Beckham, *Energy Environ Sci*, 2021, **14**, 4147-4168.
27. National Renewable Energy Laboratory (NREL), *Techno-Economic Analysis of Biochemical Scenarios for Production of Cellulosic Ethanol*, https://docs.nrel.gov/docs/fy10osti/46588.pdf.
28. National Renewable Energy Laboratory (NREL), *Process Design and Economics for Conversion of Lignocellulosic Biomass to Ethanol* https://docs.nrel.gov/docs/fy11osti/51400.pdf.
29. W. Arts, K. Van Aelst, E. Cooreman, J. Van Aelst, S. Van den Bosch and B. F. Sels, *Energy & Environmental Science*, 2023, **16**, 2518-2539.
30. Y. Liao, S. F. Koelewijn, G. Van den Bossche, J. Van Aelst, S. Van den Bosch, T. Renders, K. Navare, T. Nicolai, K. Van Aelst, M. Maesen, H. Matsushima, J. M. Thevelein, K. Van Acker, B. Lagrain, D. Verboekend and B. F. Sels, *Science*, 2020, **367**, 1385-1390.